THE ARCHIVES OF TRANSPORT

VOL. XXIV NO 2 2012

10.2478/v10174-012-0013-5

Research of Sorting Process of Unit Loads by Rotary Active Fence

Tomasz Piatkowski*
Janusz Sempruch**

Received December 2011

Abstract

The paper presents results of research of a sorting process applied to a stream of unit loads (cubiform objects, parcels) transported on conveyors. The sorting process is performed by means of an active fence (flexible arm) making above the conveyor surface the working rotary motion of one degree of freedom. The manipulated loads are treated as bodies of nonlinear elastic-damping properties described by modified nonlinear Kelvin model. The equations of motion of the flexible fence, and those of the interacting object, are derived using the finite element method. The assessment of influence of constructional and exploational parameters of the fence on the course of the sorting process and dynamic forces exerted on handled loads is the main aim of carried out investigations.

1. Introduction

The process of sorting of unit loads (e.g. postal packages) belongs to typical operations carried out in the transport centres where concentration of transported goods is high (central post offices, transit stores, airports). It consists in dividing the stream of load into new shipment directions according to the criteria recognized by the scanning system. One of the ways to perform this operation is to apply scraping devices with active arms (i.e. fences) that make rotary working motion over the belt conveyer (Fig. 1 – 3, 5, 9, 11). Such a solution (due to its uncomplicated structure) is characterized by good functionality, high strength and reliability of operation,

* University of Technology and Life Sciences, Faculty of Mechanical Engineering, ul. Kaliskiego 7, 85-796 Bydgoszcz, e–mail: topiat@utp.bydgoszcz.pl

** University of Technology and Life Sciences, Faculty of Mechanical Engineering, ul. Kaliskiego 7, 85-796 Bydgoszcz, e–mail: semjan@utp.bydgoszcz.pl

which significantly increases the overall effectiveness of the sorting system. The general knowledge of application of this type of devices (so-called nonprehensile manipulators 1, 4, 8, 2) is based only on the data contained in information booklets published by the companies specializing in producing and delivering complete distribution systems 3, 5. The contents of these booklets do not allow one to get through to the information characterising the course of the realized process of sorting, neither can one learn about imperfections of the process and their causes. There are no data that would facilitate introducing adequate changes, e.g. constructional improvements or changes in operational parameter settings, which could remove the imperfections appearing in the course of the sorting process. In order to objectively assess the basic utility features of the concept of manipulator with active fences, one undertook an attempt of developing a dynamic model of load stream distribution process. The data obtained from numerical optimisation carried out on the proposed model can be used for formulating the necessary assumptions and guidelines, applicable when one designs a manipulator with active fence satisfying concrete exploitation requirements.

2. Model of Sorting Process

For the purpose of optimization of sorting process the numerical model was build. The load (in this model) is treated as deformable body described by modified nonlinear Kelvin model 10. The static and kinetic friction forces appearing between the load and manipulator working surfaces are calculated by means of Karnopp's model 7. The resulting friction forces and moments of friction in the planar object motion on the main conveyor plane are determined according to model proposed in the work 6. Classical stiff fence (generally applied in contemporary manipulators) is replaced by flexible one – made of polyamide PA6 of constant bending strength. The flexible fence is applied to mitigate dynamic reactions exerted on the loads. This fence is treated as a continuous system discretized according to the finite element method (FEM) 14 implemented in the Matlab environment. Two-node beam elements are applied in the discrete model of the fence, in which every node is subject to translational, and rotational displacement. The driving system of manipulator puts the fence in rotary motion of angular velocity having sinusoidal course.

The continuous sorting process is considered as discrete process consisting of motion stages leading the load to the chute. These stages are activated during sorting simulation sequentially – depending on the position currently taken by the load with respect to the executing elements of manipulator. The distinguished discrete stages of the physical sorting process model are:

E1 – oblique strike of the fence against load corner,

E2 – load motion along the fence,

E3 – motion of load with one corner sliding along border of conveyor, and another one along fence,

E4 – load free motion.

Physical model of the stages characteristic for the parcel motion of the sorting process and basic equations of the mathematical model is presented in the Appendix (at the end of the paper).

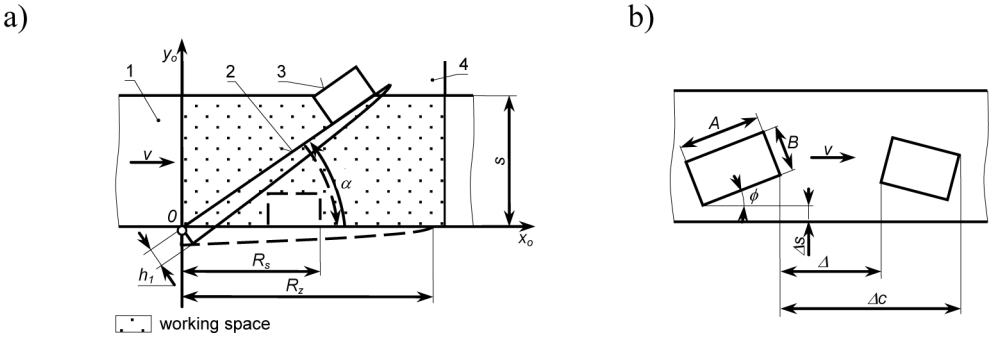

Fig. 1. Sorting process of unit load stream: a) scheme of manipulator working space, b) basic parameters of unit load stream; 1 – main conveyor, 2 – active fence, 3 – unit load, 4 – chute, v – conveyor velocity, R_z – fence length, α – fence deflection angle, h_1 – initial thickness of fence, Δc – distance between loads' fronts, Δ – distance between loads, s – conveyor width, A x B – dimensions of load, φ and Δs – load position, R_s – position of load front at starting moment of fence operation

3. Description of Optimisation Task of Sorting Process

The numerical optimization tests of sorting process are applied to assess the potential utility properties of the manipulator with an active rotary fence.The capacity maximisation of sorting process of unit load stream is the objective function of optimisation task:

$$maxQ(X) = W_t \tag{1}$$

where: $X = [R_s, v, t_1, R_z]$ – vector of decision variables, $W_t = 3600v/\Delta c$ – sorting capacity, R_s – position of load front at starting moment of fence operation (Fig. 1a), t_1 – time of fence working motion, R_z – fence length, v – conveyor velocity, Δc – distance between loads' fronts.

The distance Δc (Fig. 1b) results from requirement of continuity maintenance of the load stream supplying the manipulator and from condition of presence of only one object in working space of the fence:

$$\Delta c = \begin{cases} vt_z & \text{if} \quad vt_z > A_{\max} + \Delta \\ A_{\max} + \Delta & \text{otherwise} \end{cases} \tag{2}$$

where: A_{max} – maximal load length, Δ – distance between loads, $t_z = t_c + |R_s|/v$ – time of load scraping, $t_c = t_1 + t_2$ – time of fence working cycle, t_2 – time of fence return motion (assumed: $t_2 = t_1$).

The ranges of decision variables embrace limiting values of exploational parameters suggested in manufacturers' commercial folders of sorting devices' 3, 5 and obtained during preliminary tests of sorting process carried out by author 9, 11, 12:

$$R_s = \langle -0.5 \div 2.0 \rangle \text{m} \tag{3}$$

$$v = \langle 0.2 \div 2.5 \rangle \text{m/s} \tag{4}$$

$$t_1 = \langle 0.1 \div 1.5 \rangle \text{s} \tag{5}$$

$$R_z = \langle 0.2 \div 2.5 \rangle \text{m} \tag{6}$$

The optimization constrains take into consideration the reliability and safety requirements of sorting process course:

$$(A - R_s)/v - t_1 \leq 0 \tag{7}$$

$$-y_k + s \leq 0 \tag{8}$$

$$-T_g \leq 0 \tag{9}$$

$$w_n - w_{dop} \leq 0 \tag{10}$$

$$a_N - a_{Ndop} \leq 0 \tag{11}$$

$$\dot{y} - \dot{y}_{dop} \leq 0 \tag{12}$$

where:

y_k – maximum translocation of the object gravity centre in the chute direction,

T_g – distance between current position of load and its escaped position; this parameter relates to object of minimal size, placed by conveyor edge on opposite side in relation to fence mounting 12 – it takes into account one of more difficult sorting cases,

w_{dop} – permissible impact velocity of the load against the fence; $w_{dop} = 2.4$ m/s – velocity achieved by object during its free fall from height of $H_{dop} = 0.3$ m on undeformable ground; approx. 20% of total number of loads 13 (transported between sender and addressee) is subjected to mechanical hazard responding to fall from height of 0.3 m,

w_n – relative velocity of colliding bodies in normal direction,

$s = 0.7$ m – width of main conveyor 3, 5,

a_{Ndop} – permissible acceleration exerted on load by fence; $a_{Ndop} = 300$ m/s^2 ($\cong 30g$) – acceleration recorded during free fall test of object from height of $H_{dop} = 0.3$ m on undeformable ground 10),

g – gravity acceleration,

a_N – acceleration exerted on load by fence,

$\dot{y}_{dop}$ – permissible velocity of object leaving main conveyor towards chute; it is assumed that $\dot{y}_{dop}$ = 2.5 m/s.

During numerical optimization the stiff fence is considered. The flexible fence behaviour as the response to applied parameters of sorting process is described in section 4.3.

4. Numerical Simulation

The significant influence on decisions relating to constructional and exploational recommendations has the method arrangement of the loads' stream entered into device working space, i.e. whether the loads before the sorting process:

- occupy the arbitrary place on the whole accessible width of the main conveyor ($\Delta s \geq 0$ m – Fig. 1),
- are subjected to positioning process, in which objects are led near the conveyor border on that side, where the fence is mounted ($\Delta s = 0$ m, $\varphi = 0^o$ – Fig. 1).

In case of the first method of objects' distribution, the decisive influence on fulfilment of safety requirement of the sorted loads has the constrain (10), and in case of the second one – the constrain (11).

During sorting process simulation, two limiting cases of the gravity centre position of the object are considered simultaneously: when this centre coincides with the rear (Fig. 2a) and front corner of object (Fig. 2b). This assumption ensures correct determination of exploational and constructional parameters of manipulator (during optimization) for all objects of arbitrary distribution of mass density.

Fig. 2. Limiting cases of position of object gravity centre: a) coinciding with rear corner, b) coinciding with front corner; C_s – object gravity centre

4.1. Sorting process of loads positioned arbitrarily within the available width of the conveyor

The results of numerical optimization (consisting in capacity maximization of sorting process according to expression (1)) are presented in Fig. 3. This optimization is carried out in the function of two parameters: impact velocity w_{dop} of the load against the fence and maximal fence angle deflection α_k – taking into

consideration constrains (7)÷ (10), the friction coefficients of load with respect to carrying surfaces of conveyor $\mu_1 = 0.65$ and fence $\mu_2 = 0.35$. It is assumed that the unit load of limiting dimensions A x B = 0.7 m x 0.1 m lies just next to conveyor border (Δs = 0 m) and the object of minimal size A x B = 0.1 m x 0.1 m is moved within the longest distance from the fence (Δs = 0.6 m, s = 0.7 m). These two variants of the loads' sorting cause the most difficulty in successful object delivery to the chute.

It follows from the analysis of Fig. 3b that obtained sorting capacity is the greater, the smaller the fence deflection angle α_k. The angle α_k decrease simultaneously causes: necessity of the longer fence R_z application (Fig. 3e), the higher conveyor velocity v (Fig. 3d) and the shorter time of the fence working motion t_1 (Fig. 3a). In case of free choice of the sorting process parameters (unrestricted by range of decision variables (3)÷(6)), the optimum position of the load front (at starting moment of fence operation) should coincide with the fence rotation axis (R_s =0 m, Fig. 3c). The limitation of free choice – e.g. upper limit achievement of range variable v (4) – extorts the fence motion activation delay (i.e. the distance R_s enlargement – Fig. 3c) at the cost of sorting capacity W_t (Fig. 3b). The graph of the required distance Δ between sorted objects is presented in Fig. 3f. This graph is worked out on the basis of parameters t_1, R_s, v (Fig. 3a, c, d) and expression (2).

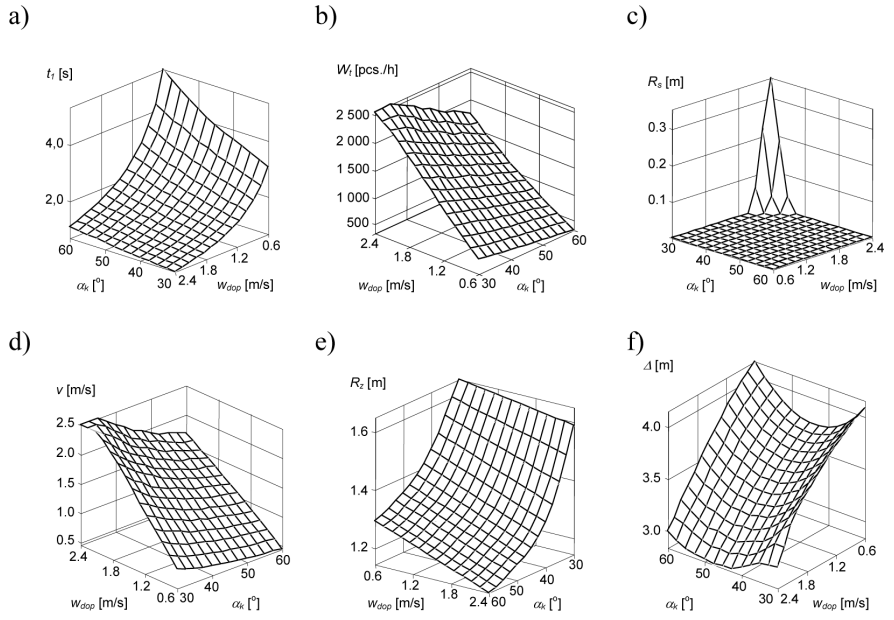

Fig. 3. Manipulator working parameters in function of impact velocity w_{dop} of the object against the fence and maximal angle α_k of fence deflection, taking into account constrains (7)÷(10): a) time of fence working motion, b) sorting capacity, c) load's front position at starting moment of fence operation, d) conveyor velocity, e) fence length, f) required distance between loads

The influence of friction coefficients μ_1 and μ_2 on the exploational parameters of manipulator with the rotary fence is shown in Fig. 4. It is assumed that: A x B = 0.7 m x 0.1 m and A x B = 0.1 m x 0.1 m, H_{dop} = 0.3 m (w_{dop} = 2.4 m/s), α_k = 40°, R_s = 0 m, R_z = 1.4 m, s = 0.7 m and extreme distribution of object mass density (see Fig. 2a and b). Sorting capacity is the greater, the smaller values of friction coefficients μ_1 and μ_2 (Fig. 4b). An increase of sorting capacity is achieved thanks to easier object displacement along the fence towards chute (when the values of μ_1 and μ_2 are small). It enables the conveyor velocity v decrease (Fig. 4c) and time t_1 of the fence working motion shortening (Fig. 4a).

The influence of load length A on the course of sorting process is shown in Fig. 5. Presented data are obtained on the basis of numerical optimization consisting in maximization of sorting capacity (1) which takes into consideration constrains (7)÷(10) and assumptions: B = 0.1 m, α_k = 40°. The lengthier load, the smaller sorting capacity is achieved (Fig. 5a) and greater fence length R_z is required (Fig. 5c). The sorting capacity decrease (in case of greater load length A) is caused by lengthier fence application necessity, which leads to the fence rotation velocity decrease (i.e. time t_1 increase – according to constrain (10)).

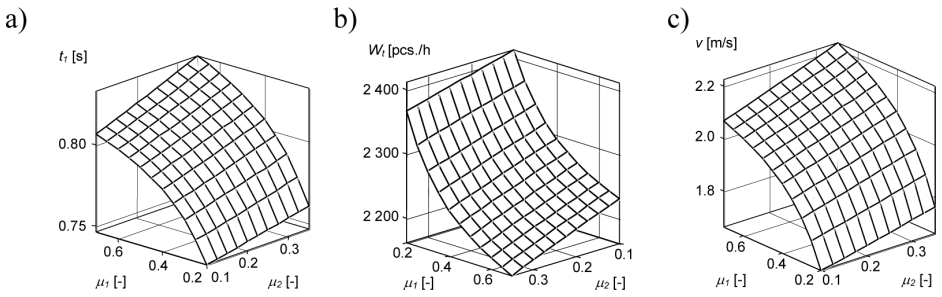

Fig. 4. Manipulator working parameters in function of friction coefficients μ_1 and μ_2: a) time of fence working motion, b) sorting capacity, c) conveyor velocity

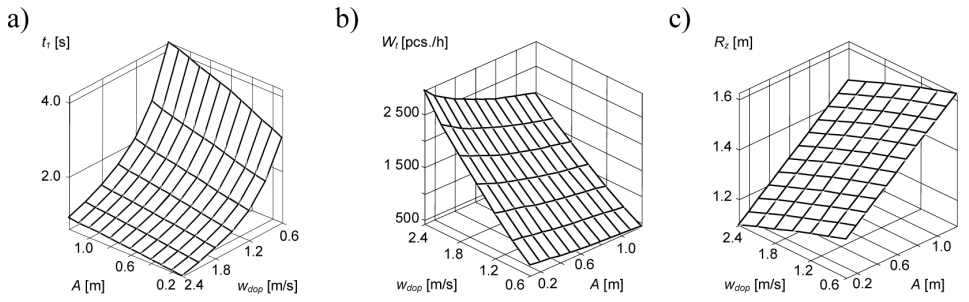

Fig. 5. Manipulator working parameters in function of load length A and impact velocity w_{dop} of the load against fence: a) sorting capacity, b) load's front position at starting moment of fence operation, c) fence length

4.2. Sorting process of loads positioned next to conveyor border on fence mounting side

The results of numerical optimization concerning capacity maximization of sorting process according to expression (1) and constrains (7), (8), (11) are shown in Fig. 6. Presented data are determined in the function of the fence deflection angle α_k and acceleration a_{Ndop} exerted on object – assuming: load dimensions A x B = 0.7 m x 0.1 m and friction coefficients: μ_1 = 0.65 i μ_2 = 0.35. It follows on the analysis of Fig. 6, that load positioning (before their sorting) next to conveyor border on that side, where the fence is mounted (Δs = 0 m) contributes to the shorter fence application (Fig. 6e) in comparison with arbitrary objects' arrangement on the conveyor (Fig. 3e). If the object is subjected to higher accelerations, the fence activation should be at the moment when the object is already partly in the manipulator working space – R_s>0, Fig. 6c. When the object is subjected to the smaller dynamic interactions, the lower values of fence angle a_k deflection are conducive to increase of sorting capacity W_t (Fig. 6b). This relationship changes, if the object is subjected to the higher admissible acceleration. The sorting capacity W_t is then the greater,

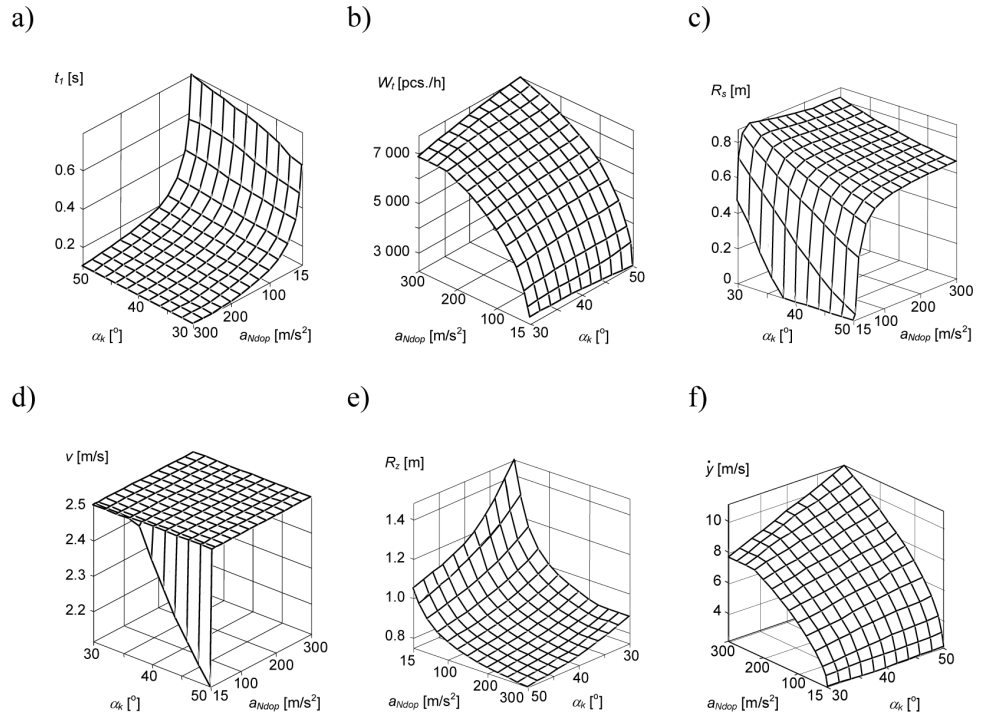

Fig. 6. Manipulator working parameters in function of maximal angle α_k of the fence deflection and acceleration a_{Ndop} exerted on the load, taking into consideration constrains (7), (8) and (11): a) time of fence working motion, b) sorting capacity, c) load's front position at starting moment of fence operation, d) conveyor velocity, e) fence length, f) velocity of object leaving main conveyor towards chute, when gravity mass centre is placed according to Fig. 2b

the greater angle α_k. The maximum of capacity (W_t =8000 pcs./h) is achieved when time t_1 of the fence working motion (Fig. 6a) obtains the bottom range limit of decision variable's (5) and the conveyor velocity v (Fig. 6d) coincides with upper limit of admissible range (4). This working parameters cause achievement of object acceleration a_N = 300 m/s^2 ($\cong 30g$) and very high velocity of sorted load entered to the chute – above 10 m/s (Fig. 6f).

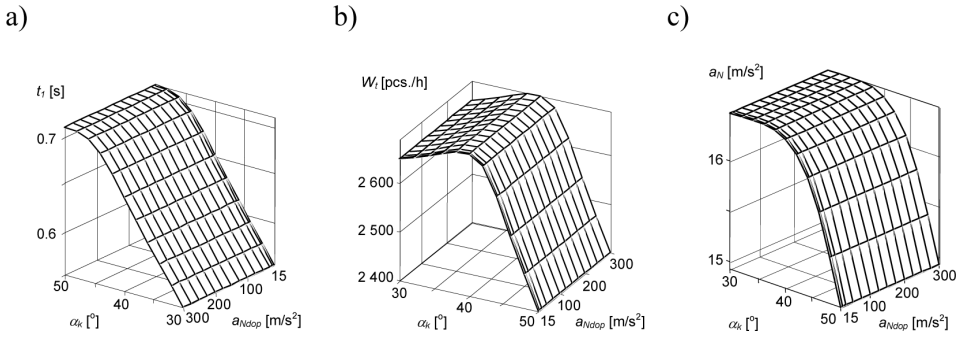

Fig. 7. Results of numerical optimization, taking into consideration constrain (12) and data applied during preparation of Fig. 6: a) time of fence working motion, b) sorting capacity, c) acceleration exerted on the load

The constraint (12) application has an influence on: elongation of the time of the fence working motion (Fig. 7a), capacity decrease (Fig. 7b) and change of the relationship between capacity W_t and the angle α_k of fence deflection. Maximum capacity W_t = 2700 pcs./h is achieved, when the angle α_k = 40° and t_1 = 0.65 s. Maximum acceleration exerted on the load doesn't exceed 17 m/s^2 (Fig. 7c).

The graphs shown in Fig. 8 present the influence of the load length A of minimum width B = 0.1 m and admissible object accelerations a_{Ndop} on the capacity maximization of the sorting process (assuming: α_k = 40°, μ_2 = 0.65 and μ_2 = 0.35). The non-uniform distribution of load mass density is also taken into consideration (according to Fig. 2a, b) – similarly like during preparation of Fig. 3÷Fig. 7.

In case of small acceleration exerted on the load (a_{Ndop} < 15 m/s^2 $\cong$ $1.5g$), the difference between sorting capacity of short objects (A = 0.1 m) and long ones (A = 1.2 m) is insignificant (Fig. 8b). This difference is definitely greater, when the object can be subjected to high acceleration. If the mass centre coincides with the front of loads and maximal sorting capacity is applied (W_t = 14000 pcs./h, Fig. 8b), the considerable velocity of objects leaving the main conveyor is achieved (particularly in case of long objects – approx. $\dot{y}$ = 12 m/s, Fig. 9). This velocity limitation (to 2.5 m/s – constrain (12)) causes time elongation of the fence working motion (Fig. 10a) and sorting capacity decrease: in case of long objects to approx. W_t = 2000 pcs./h (Fig. 10b), and in case of short objects (A = 0.1 m) only to approx. W_t = 12000 pcs./ h.

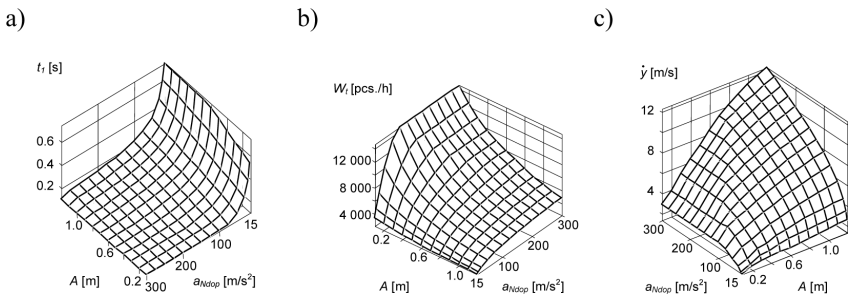

Fig. 8. Manipulator working parameters in function of load length A and acceleration a_{Ndop} exerted on the load, taking into consideration constrains (7), (8) and (11): a) time of fence working motion, b) sorting capacity, c) load's front position at starting moment of fence operation

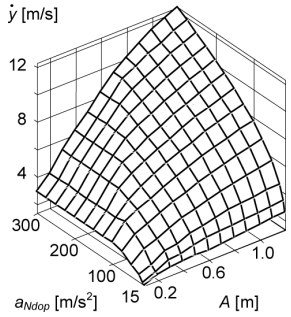

Fig. 9. Velocity of object leaving main conveyor towards chute, when gravity mass centre is placed according to Fig. 2b

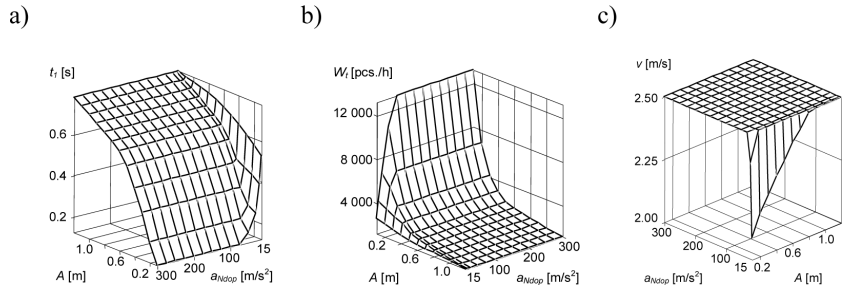

Fig. 10. Results of numerical optimization, taking into consideration constrain (12) and data applied during preparation of Fig. 8: a) time of fence working motion, b) sorting capacity, c) conveyor velocity

4.3. The analysis of flexible fence influence on acceleration exerted on the sorted objects

During numerical tests, the fence of constant bending strength is considered, made of polyamide PA6 (z x h_1 x R_z =0.1 m x 0.08 m x 1.2 m, Fig. 1a; z – the fence height). It is also assumed that: maximum deflection of the fence tip will not exceed 0.08 m, s =0.7 m, μ_1 =0.65, μ_2 =0.35, b_p =3.3·10^5 Nskg$^{-0.4}$m^{-3}, k_p =1.72·10^9 Nm^{-4} (b_p, k_p – the coefficients of damping and stiffness of the load, according to 10). The manipulator working parameters are so chosen to cause impact velocity between the fence and object as during body free fall from height H = 0.3 m (treated as the admissible impact velocity).

The courses of dynamic processes that take place when the object (m_p =15 kg) impacts against the fence are presented in Fig. 11. The point 1 marked in the graphs pertains to the moment of impact initiation, while the point 2 denotes the end of impact. The point where object loses its contact with the fence lies out of the main conveyor area, Fig. 11a.

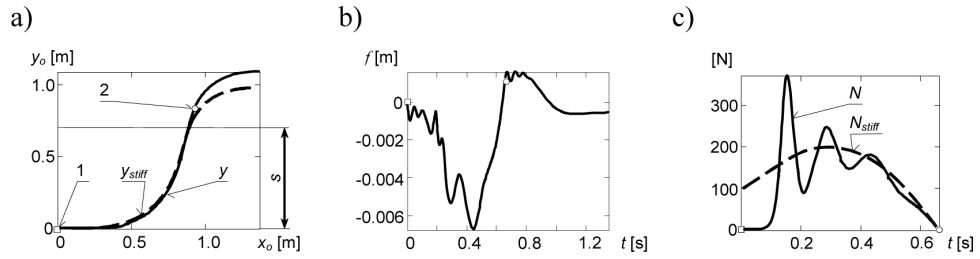

Fig. 11. Results of simulation of the object impact against the fence (1 and 2 – beginning and end of impact, respectively): a) motion trajectory of object's gravity centre, b) deflection of fence tip, c) course of dynamic reactions during impact of load against flexible fence (N), and against undeformable obstacle of infinite mass (N_{stiff})

The oscillatory motion of the fence fades down before the fence returns to its initial position (Fig. 11b), owing to which the following working cycles are free of disturbances that might result from the transients of previous cycles. The courses of dynamic reactions presented in Fig. 11c relates to the impact appearing between the object and the flexible fence (N), and between this object and an undeformable obstacle of infinite mass (N_{stiff}). It follows from the analysis of the obtained results that, during the impact of the object against the flexible fence, one can expect almost threefold decrease of dynamic reactions compared to those appearing when the object impacts against an undeformable, immobile obstacle (the one which represents a completely rigid fence joined with a rigid drive system; such a fence exerts most destructive effect on the manipulated loads).

The course of sorting process for the object which, before scrapping, lies near the border of conveyor (Δs = 0) is shown in Fig. 12. The fence constructional parameters coincide with parameters applied in Fig. 11. The reference mark 1 indi-

cates the moment of initiation of contact between the object and the fence, and the reference mark 2 – the end of this contact.

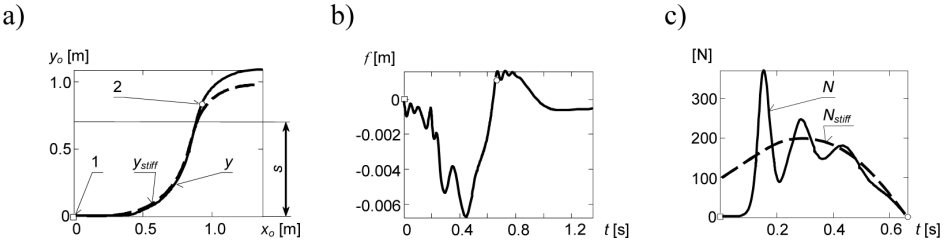

Fig. 12. Results of simulation of object's motion along fence (1 – initiation of contact between object and fence, 2 – beginning of free motion of object): a) motion trajectory of gravity centre of object, b) deflection of fence tip, c) courses of dynamic interactions between object and flexible fence (N), and between object and stiff fence (N_{stiff})

The results of simulations for a stiff fence put in motion by a stiff drive system (curves denoted with a dashed line, Fig. 12a) are used as a reference for the results of tests carried out with the use of a flexible fence. An object moving along a flexible fence is given a higher displacement in transverse direction of the belt than that achieved in case of a stiff fence (Fig. 12a). In case of object motion along the fence, dynamic force exerted on the object (Fig. 12c) is decidedly smaller than during its impact against the fence (Fig. 11c). Deflection of the fence end is also smaller (Fig. 12b). It results, that the selection of manipulator structural features should be made on the basis of the analysis of sorting process, which can be reduced to examining the stage of oblique impact between the object and the fence. The design that ensures the ability to mitigate the dynamic reactions appearing during the impact of manipulated object against the fence also makes it possible to achieve correct execution of other stages of the sorting process – including the stage of object's motion along the fence.

5. Conclusions

The analysis of simulation testing results of sorting process of unit load stream indicates that:

- the flexible fence application mitigates dynamic reactions exerted on objects (during impact) – without loss of course correctness of sorting process,
- the loads' stream positioning (before sorting) just next to conveyor border (at the side where the fence is mounted) enables to obtain greater efficiency of sorting capacity (especially of short objects) than in case of arbitrary arrangement of loads within the available width of the conveyor,
- the friction properties of carrying surfaces of the fence and conveyor should be as small as possible – independently of the method of the loads arrangement

on the conveyor before sorting; the smaller friction coefficient of these surfaces, the greater sorting efficiency,

- sorting process parameters depend on the method of an arrangement of the loads entered into working space of manipulator:
  - when the sorted loads are arbitrary situated on the conveyor:
    - optimum angle of maximal fence deflection is $\alpha_k = 35^\circ$,
    - fence operation should start at the moment when the load front crosses the axis of the fence rotation ($R_s = 0$ m) – independently of applied fence length R_z, maximal angle α_k of fence deflection and conveyor velocity v,
  - when the sorted loads are situated next to conveyor border at the side of fence mounting:
    - optimum angle of maximal fence deflection is $\alpha_k = 40^\circ$,
    - the activation R_s of working motion of the fence is not constant value – it depends on conveyor transportation velocity v, maximal angle α_k of fence deflection and loads' dimensions.

APPENDIX

Physical Model of the Sorting Process and Basic Equations of the Mathematical Model

Four reference coordinate systems were assumed in determining the equations of the physical model (Fig. 13÷Fig. 17):

- rectangular Ox_0y_0, connected with the manipulator's frame, whose origin lies on the fence rotation axis – this one was applied in presentation of the results of load motion simulation,
- rectangular Oy_pz_p, connected with the load – applied for determining the position of the load's gravity centre with respect to its geometric centre,
- rectangular Ox_3x_1, connected with a specific discrete element – applied in description of physical properties of discrete elements of the fence,
- polar coordinate system, with radius-vector r and polar angle α_p – applied in deriving the equations of load motion.

E1 – oblique impact of the load against the fence

The system of equations of forces and moments, acting on the load and the fence:

$$\begin{cases} M_b\ddot{q} + B_b\dot{q} + K_bq = Q \\ m_p\ddot{r} = F_\xi + P_{cen} - F_2\cos\left(\alpha_p - q_{5(N)}\right) + N\sin\left(\alpha_p - q_{5(N)}\right) \\ m_pr\ddot{\alpha}_p = -F_\eta - P_{Cor} + F_2\sin\left(\alpha_p - q_{5(N)}\right) + N\cos\left(\alpha_p - q_{5(N)}\right) \\ I_p\ddot{\varphi} = -r_{Cj}\left[u_jN\cos\left(\gamma_j + u_j(\varphi - q_{5(N)})\right) + F_2\sin\left(\gamma_j + u_j(\varphi - q_{5(N)})\right)\right] - T \end{cases} \tag{13}$$

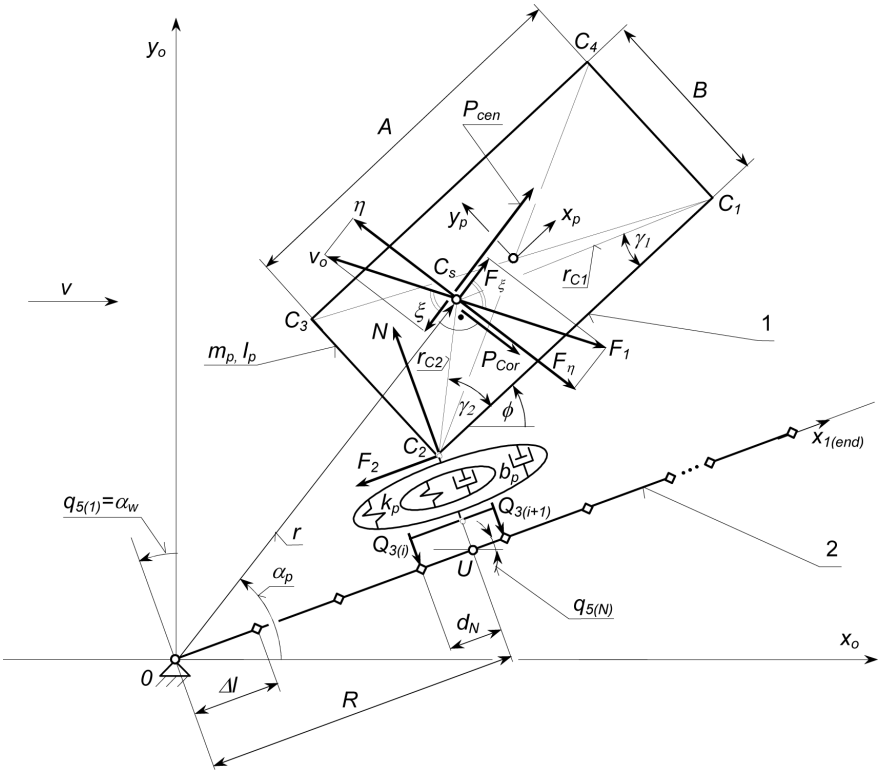

Fig. 13. Scheme of forces acting on load during its impact against active fence; 1 – load, 2 fence

where:

j = 1,2,3,4 – number of load's corner being in contact with fence,

i = 1,2,3...n_E+1 – number of node of fence's discrete element being in contact with load (according to Fig. 14),

n =2(n_E+1) – number of degrees of freedom of nodes in fence's discrete model,

n_E –number of discrete elements,

M_b, B_b, K_b – matrices of inertia, damping and rigidity of fence's discrete model, of dimensions nxn,

q – vector of generalized displacements of nodes, of dimensions nx1,

Q – vector of generalized forces acting on nodes of discrete elements, of dimensions nx1,

$q_{5(N)}$ – angular position of fence's discrete element at its contact point with load U – according to Equation (32),

$Q_{3(i)}$ – external force exerted on i-th node of discrete element,

$q_{5(1)} = \alpha_w$ – angular position of first node of discrete element,

m_p, I_p – load mass and mass moment of inertia,

φ – rotation angle of load,

P_{Cor}, P_{cen} – Coriolis force and centrifugal force:

$$P_{Cor} = 2m_p\dot{\alpha}_p\dot{r} \tag{14}$$

$$P_{cen} = m_p\dot{\alpha}_p^2 r \tag{15}$$

N – force of reaction between load and fence in normal direction of impact 10:

$$N = b_p m_p^{0,4}\dot{D}D^2 + k_p D^4 \tag{16}$$

b_p, k_p – damping [Nskg$^{-0,4}$m^{-3}] and stiffness [Nm^{-4}] factors.

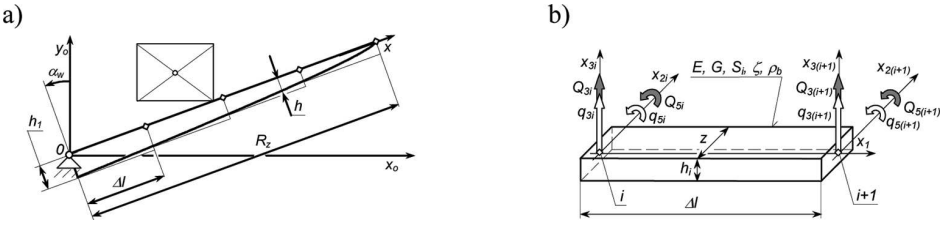

Fig. 14. Division of fence's flexible link into discrete FEMs: a) discrete model of fence, b) two-node discrete beam model; q_3, q_5 – generalized coordinates (two degrees of freedom: translation and rotation), Q_3, Q_5 – generalized forces, E – Young's modulus, G – shear (Kirchhoff's) modulus, $S_i = zh_i$ – area of transverse cross-section, ζ – material damping, ρ_b – mass density, α_w – angular position of fence's driving link, Δl – length of discrete element, R_z – length of fence, h_1 – initial thickness

The first equation in system (13) is a matrix equation of motion of discrete elements of the fence. The remaining equations describe motion of the load in the polar coordinate system with radius-vector r and polar angle α_p.

Depending on which of the load's corners C_j is in contact with the fence, the length of radius-vector r_{Ci} connecting the corner C_j (j = 1,2,3,4) with gravity centre of the load C_s is equal to

$$r_{Cj} = \begin{cases} \sqrt{\left(0.5A + (3-j)x_p\right)^2 + \left(0.5B + (3-j)y_p\right)^2} & \text{if} \quad j = 2,4 \\ \sqrt{\left(0.5A - (2-j)x_p\right)^2 + \left(0.5B + (2-j)y_p\right)^2} & \text{otherwise} \end{cases} \tag{17}$$

The position angle of load's gravity centre γ_j is defined by the relationship:

$$\gamma_j = \begin{cases} arc\ \sin\left(\dfrac{0,5B + y_p}{r_{Cj}}\right) & \text{if} \quad j = 1,2 \\ arc\ \sin\left(\dfrac{0,5B - y_p}{r_{Cj}}\right) & \text{otherwise} \end{cases} \tag{18}$$

and the factor u_j appearing in Equations (13) is defined as

$$u_j = \begin{cases} 1 & \text{if} \quad j = 2,4 \\ -1 & \text{otherwise} \end{cases} \tag{19}$$

For the reaction force N between the object and the load be continuously and uniformly transmitted, one assumes that adjacent nodes of discrete elements are simultaneously subjected to adequately reduced generalized forces $Q_{3(i)}$ and $Q_{3(i+1)}$, according to the following proportions:

$$Q_{3(i)} = N\left(1 - \frac{d_N}{\Delta l}\right), \quad Q_{3(i+1)} = N\frac{d_N}{\Delta l} \tag{20}$$

where:

$\Delta l = R_z/n_E$ – length of discrete element,

R_z – –length of fence.

Assuming that the deflection angle of fence (under the pressure of object – Fig. 13), the number of the fence's discrete element being in contact with the object can be determined as the integer portion of the quotient of R and Δl:

$$i = \begin{cases} E\left(\dfrac{R}{\Delta l}\right) + 1 & \text{if} \quad E\left(\dfrac{R}{\Delta l}\right) + 1 < n_{OES} \\ \text{error} & \text{otherwise} \end{cases} \tag{21}$$

and the segment dN is the reminder of this quotient:

$$d_N = \operatorname{mod}\left(\frac{R}{\Delta l}\right) \tag{22}$$

The distance between the corner C_j and rotation axis of the fence is given by formula:

$$R = \sqrt{x_{oC}^2 + y_{oC}^2} \tag{23}$$

where the coordinates x_{oC}, y_{oC} of point C_j can be expressed as:

$$x_{oC} = r\cos\alpha_p - u_j r_{Cj}\cos(\gamma_j + \varphi) \tag{24}$$

$$y_{oC} = r\sin\alpha_p - r_{Cj}\sin(\gamma_j + \varphi) \tag{25}$$

Deformation of the load at the contact point C_j in normal impact direction (necessary for determining the reaction force N) is the shortest distance between the fence and the load's corner. This distance is defined by the length of segment connecting the points C_j and U (see Fig. 13)

$$D = \frac{y_{oU} - y_{oC}}{\cos q_{5(N)}} \tag{26}$$

The point U lying on the surface of fence is determined based on the assumption that, as the fence deflects making its rotary motion, the distance Δl between adjacent nodes of discrete elements remains constant, and translation dislocations of the nodes

q_3 are represented by the arches drawn by the ends of discrete elements – as shown in Fig. 15. The coordinates of point U are:

$$x_{oU} = d_N \cos\vartheta_N + \sum_{k=1}^{i-1} \Delta l \cos\vartheta_k \tag{27}$$

$$y_{oU} = d_N \sin\vartheta_N + \sum_{k=1}^{i-1} \Delta l \sin\vartheta_k \tag{28}$$

where:

ϑ_k – angle between straight line passing through nodes k and $k+1$ and abscissa axis of Ox_oy_o system – Fig. 15:

$$\vartheta_k = \frac{q_{3(k+1)} - q_{3(k)}}{\Delta l} \tag{29}$$

ϑ_N – angle between straight line passing through points U and node i and abscissa axis of Ox_oy_o system:

$$\vartheta_N = \frac{q_{3(N)} - q_{3(i)}}{d_N} \tag{30}$$

$q_{3(N)}$, $q_{5(N)}$ – coordinates of point U in rectangular coordinate system Ox_3x_1, calculated on the basis of polynomial approximation of dislocation within discrete elements 14:

$$q_{3(N)} = q_3(d_N) = p_1 + p_2 d_N + p_3 d_N^2 + p_4 d_N^3 \tag{31}$$

$$q_{5(N)} = q_5(d_N) = p_2 + 2p_3 d_N + 3p_4 d_N^2 \tag{32}$$

$p = [p_1, p_2, p_3, p_4]$ – vector of coefficients determined on the basis of boundary conditions $q_3(0)$, $q_5(0)$, $q_3(\Delta l)$ and $q_5(\Delta l)$ substituted into Equations (31) and (32).

The speed of load deformation during the impact can be written as

$$\dot{D} = \frac{d}{dt}(D) \tag{33}$$

The friction forces exerted on the load can be expressed as 7, 6:

$$F_\xi = \begin{cases} \dfrac{\xi F_{\max}}{v_o \sqrt{1 + \left(\frac{T_{\max}\dot{\varphi}}{F_{\max} v_o}\right)^2}} & \text{if} \quad v_o > v_{\min} \\ \begin{cases} P_{\xi ext} & \text{if} \quad F_{\max} > P_{1ext} \\ F_{\max} \dfrac{P_{\xi ext}}{P_{1ext}} & \text{otherwise} \end{cases} & \text{otherwise} \end{cases} \tag{34}$$

$$F_\eta = \begin{cases} \dfrac{\eta F_{\max}}{v_o \sqrt{1 + \left(\frac{T_{\max}\dot{\varphi}}{F_{\max} v_o}\right)^2}} & \text{if} \quad v_o > v_{\min} \\ \begin{cases} P_{\eta ext} & \text{if} \quad F_{\max} > P_{1ext} \\ F_{\max} \dfrac{P_{\eta ext}}{P_{1ext}} & \text{otherwise} \end{cases} & \text{otherwise} \end{cases} \tag{35}$$

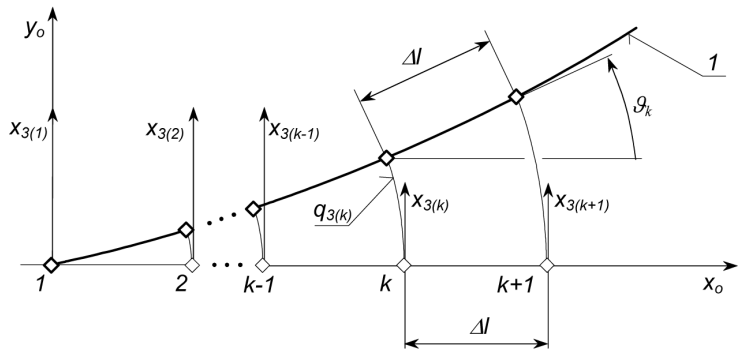

Fig. 15. Interpretation of translational displacements of discrete element nodes of fence moving in rotational motion; 1 – fence, $q_{3(k)}$ – translational displacement of node k

$$T = \begin{cases} \dfrac{T_{\max} sgn(\dot{\varphi})}{\sqrt{1 + \left(\frac{F_{\max} v_o}{T_{\max} \dot{\varphi}}\right)^2}} & \text{if} \quad |\dot{\varphi}| > \dot{\varphi}_{\min} \\ \begin{cases} T_{ext} & \text{if} \quad T_{\max} > |T_{ext}| \\ T_{\max} sgn(T_{ext}) & \text{otherwise} \end{cases} & \text{otherwise} \end{cases} \tag{36}$$

$$F_2 = \begin{cases} N\mu_2 sgn(w_{xj}) & \text{if} \quad |w_{xj}| > v_{\min} \\ \begin{cases} P_{2ext} & \text{if} \quad N\mu_2 > |P_{2ext}| \\ N\mu_2 sgn(P_{2ext}) & \text{otherwise} \end{cases} & \text{otherwise} \end{cases} \tag{37}$$

where:

F_{max}, T_{max} – maximal friction force and maximal friction moment appearing in the case of pure translational, or pure rotational motion of load,

$v_{\min} = 10^{-6}$ m/s, $\dot{\varphi}_{\min} = 10^{-6}$ rad/s – assumed threshold speed, below which the rubbing speed is considered zero 7,

P_{1ext} – resultant external force exerted by fence on object

$$P_{1ext} = \sqrt{P_{\xi ext}^2 + P_{\eta ext}^2} \tag{38}$$

$P_{\xi ext}$, $P_{\eta ext}$ – components of force P_{1ext}:

$$P_{\xi ext} = N\left(\mu_2 sgn(w_{xj}) \cos\left(\alpha_p - q_{5(N)}\right) - \sin\left(\alpha_p - q_{5(N)}\right)\right) \tag{39}$$

$$P_{\eta ext} = N\left(\mu_2 sgn(w_{xj}) \sin\left(\alpha_p - q_{5(N)}\right) + \cos\left(\alpha_p - q_{5(N)}\right)\right) \tag{40}$$

T_{ext} – moment of external forces exerted on object:

$$T_{ext} = -r_{Cj} N \left[\begin{array}{l} u_j \cos\left(\gamma_j + u_j(\varphi - q_{5(N)})\right) + \\ +\mu_2 sgn(w_{xj}) \sin\left(\gamma_j + u_j(\varphi - q_{5(N)})\right) \end{array} \right] \tag{41}$$

P_{2ext} – external force, tangent to fence, exerted by frictional coupling existing between object and carrying surface of conveyor:

$$P_{2ext} = F_\xi \cos(\alpha_p - q_{5(N)}) + F_\eta \sin(\alpha_p - q_{5(N)}) \tag{42}$$

μ_1, μ_2 – friction coefficients of load with respect to belt of conveyor and fence,

w_{xj}– speed of sliding of load's corner with respect to fence:

$$\begin{aligned} w_{xj} = {} & \dot{r}\cos\left(\alpha_p - q_{5(N)}\right) - r\left(\dot{\alpha}_p - \dot{q}_{5(N)}\right)\sin\left(\alpha_p - q_{5(N)}\right) + \\ & + r_{Cj}\left(\dot{\varphi} - \dot{q}_{5(N)}\right)\sin\left(\gamma_j + u_j(\varphi - q_{5(N)}\right) \end{aligned} \tag{43}$$

The values of components ζ and η of the vector of relative friction speed v_o of the load's gravity centre C_s on the conveyor belt are equal to:

$$\xi = v\cos\alpha_p - \dot{r} \tag{44}$$

$$\eta = v\sin\alpha_p + r\dot{\alpha}_p \tag{45}$$

E2 – motion of load along fence

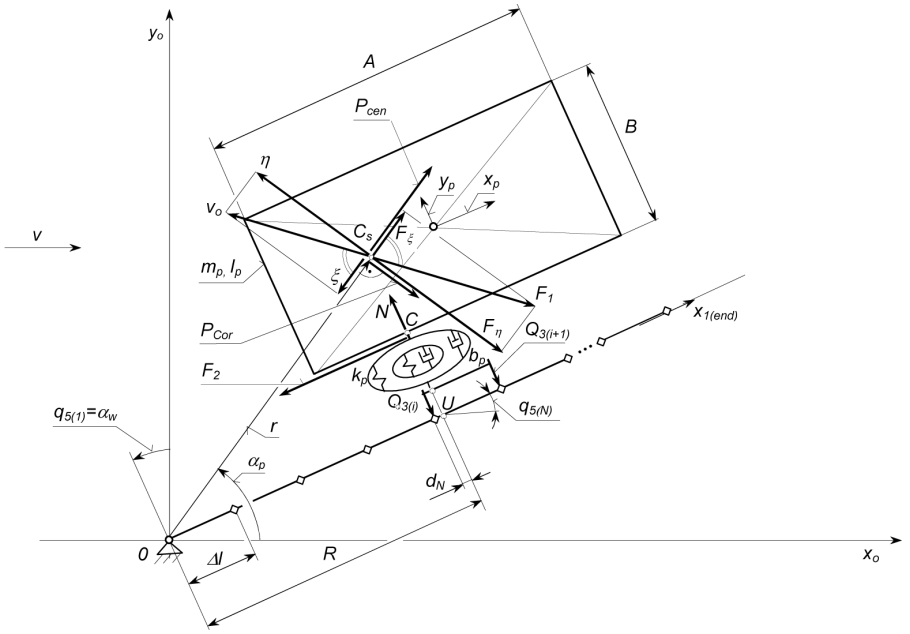

Fig. 16. Scheme of forces acting on load moving along the fence

Dynamic interactions between the load and the fence can be expressed by the equations (according to Fig. 16)

$$\begin{cases} M_b\ddot{q} + B_b\dot{q} + K_b q = Q \\ m_p\ddot{r} = F_\xi - F_2\cos\left(\alpha_p - q_{5(N)}\right) + N\sin\left(\alpha_p - q_{5(N)}\right) + P_{cen} \\ m_p r\ddot{\alpha}_p = F_2\sin(\alpha_p - q_{5(N)}) + N\cos\left(\alpha_p - q_{5(N)}\right) - F_\eta - P_{Cor} \end{cases} \tag{46}$$

Denotations of quantities used in these equations are the same as those in Equations (13).

The reaction forces between the object and the fence are applied at the point C, which is a rectangular projection of the object's centre of gravity C_s on the wall of load that touches the fence.

Deformation and deformation speed of the load at the contact point C in normal impact direction (necessary for determining the reaction force N) are described according to equations (26)÷(33).

The external forces $P_{\xi ext}$, $P_{\eta ext}$ and P_{2ext} exerted on the object (required for determining the force of friction according to Equations (34), (35) and (37)) take the form of equations (39), (40) and (42).

The sliding speed of the object with respect to the fence, which appears in Equation (37), is

$$w_x = \dot{r}\cos\left(\alpha_p - q_{5(N)}\right) - r(\dot{\alpha}_p - \dot{q}_{5(N)})\sin\left(\alpha_p - q_{5(N)}\right) \tag{47}$$

The coordinates of point C, necessary for determining the distance R from the i-th node of the fence's discrete element being in contact with the object, are equal to (according to Fig. 16):

$$x_{oC} = r\cos\alpha_p + (0.5B + y_p)\sin q_{5(N)} \tag{48}$$

$$y_{oC} = r\sin\alpha_p - (0.5B + y_p)\cos q_{5(N)} \tag{49}$$

E3 – motion of load with one corner sliding along border of conveyor, and another one along fence

If the load lies just next to conveyor border (at the side where the fence is mounted), it may cause slide of one load's corner along the border of conveyor, and another one along the fence (Fig. 17). Then, the load is lead out from the stream of loads in the result of impact-free sliding along the fence.

The load and fence motions can be described by the following equations:

$$\begin{cases} M_b\ddot{q} + B_b\dot{q} + K_b q = Q \\ m_p\ddot{r} = F_\xi + P_{cen} + N_2\sin\alpha_p - F_{2(2)}\cos\alpha_p + N_1\sin\left(\alpha_p - q_{5(N)}\right) + \\ \quad -F_{2(1)}\cos\left(\alpha_p - q_{5(N)}\right) \\ m_p r\ddot{\alpha}_p = -F_\eta - P_{Cor} + N_2\cos\alpha_p + F_{2(2)}\sin\alpha_p + N_1\cos\left(\alpha_p - q_{5(N)}\right) + \\ \quad +F_{2(1)}\sin\left(\alpha_p - q_{5(N)}\right) \\ I_p\ddot{\varphi} = r_{C1}\left[N_1\cos\left(q_{5(N)} + \gamma_1 - \varphi\right) - F_{2(1)}\sin\left(q_{5(N)} + \gamma_1 - \varphi\right)\right] + \\ \quad -r_{C2}\left[N_2\cos\left(\gamma_2 + \varphi\right) + F_{2(2)}\sin\left(\gamma_2 + \varphi\right)\right] - T \end{cases} \tag{50}$$

In case of static friction between the load and the conveyor, the reaction forces and the moments exerted on the object (required in Equations (34)÷(36)) take the form:

$$P_{\xi ext} = -N_2\sin\alpha_p + F_{2(2)}\cos\alpha_p - N_1\sin(\alpha_p - q_{5(N)}) + F_{2(1)}\cos(\alpha_p - q_{5(N)}) \tag{51}$$

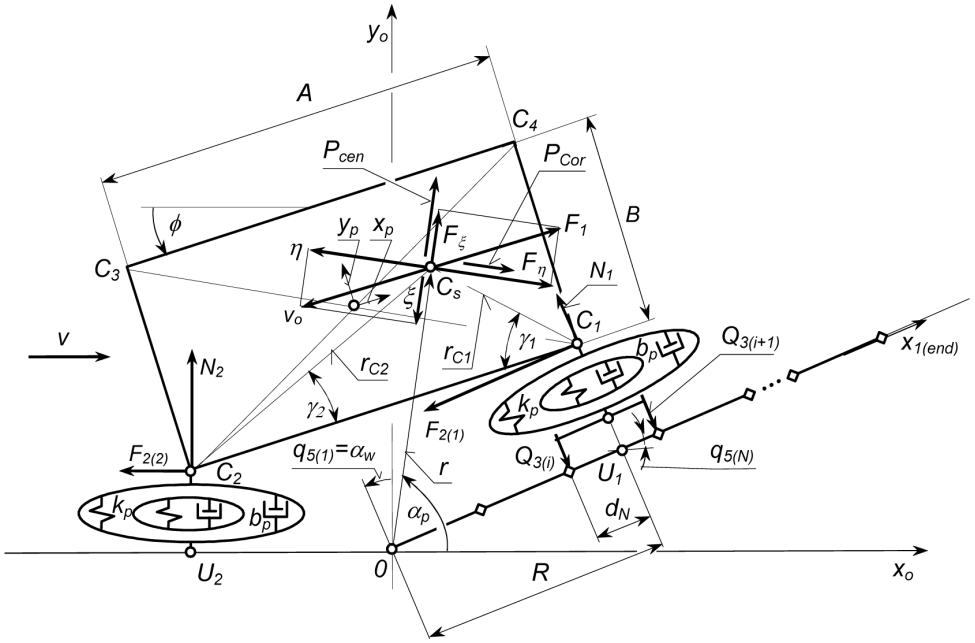

Fig. 17. Scheme of forces acting on load whose one corner rubs against border of conveyor, and another one against fence

$$P_{\eta ext} = N_2 \cos\alpha_p + F_{2(2)} \sin\alpha_p + N_1 \cos(\alpha_p - q_{5(N)}) + F_{2(1)} \sin(\alpha_p - q_{5(N)}) \quad (52)$$

$$\begin{aligned} T_{ext} = {} & r_{C1} \left[N_1 \cos\left(q_{5(N)} + \gamma_1 - \varphi\right) - F_{2(1)} \sin\left(q_{5(N)} + \gamma_1 - \varphi\right) \right] + \\ & - r_{C2} \left[N_2 \cos\left(\gamma_2 + \varphi\right) + F_{2(2)} \sin\left(\gamma_2 + \varphi\right) \right] \end{aligned} \quad (53)$$

The sliding speeds of the object's corners, w_{x1} – referred to the fence at the contact point C_l and w_{x2} – referred to conveyor border at point C_2, are given by equations:

$$\begin{aligned} w_{x1} = {} & \dot{r} \cos(\alpha_p - q_{5(N)}) - r(\dot{\alpha}_p - \dot{q}_{5(N)}) \sin(\alpha_p - q_{5(N)}) + \\ & + r_{C1}(\dot{\alpha}_p - \dot{q}_{5(N)}) \sin(\alpha + \gamma_1 - \varphi) \end{aligned} \quad (54)$$

$$w_{x2} = \dot{r} \cos\alpha_p - r\dot{\alpha}_p \sin\alpha_p + r_{C2}\dot{\varphi} \sin(\gamma_2 + \varphi) \quad (55)$$

Due to the conditions existing during sorting, these speeds take values greater than zero – which was confirmed in preliminary investigations. For this reason, we assume that only kinetic friction exists at points C_j (j =1,2), and $F_{2(j)} = N_{(j)}\mu_2$– according to Equation (37).

Deformation of the object at the contact point C_2 is

$$D = -y_{oC2} \quad (56)$$

where:

y_{oC2} – ordinate of point C_2 in coordinate system Ox_oy_o.

The remaining denotations are the same, as those in description of Equations (13).

References

1. Akella S., Huang W.H., Lynch K.M., Mason, M.T.: Parts feeding on a conveyor with a one joint robot. Algorithmica 26, 2000, 313-344.
2. Akella S., Mason M.T.: Posing polygonal objects in the plane by pushing. The International Journal of Robotics Research 17, 1998, 70-88.
3. Autosort 4 – Flat Face Arm Sorter, accessed 2010-10-19, Commercial folder published by Automation Inc., Oak Lawn, IL, USA, www.automotionconveyors.com/ media/print_media/products/ sc4_flatface.pdf.
4. Berretty R.P., Goldberg K.Y., Overmars M.H., Stappen A.F.: Computing fence designs for orienting parts. Computational Geometry 10, 1998, 249-262.
5. Flat Belt Sorter, accessed 2007-10-27, Commercial folder published by Sandvik Materials Technology, Sandviken, Sweden. www.sorting.com.
6. Goyal S., Ruina A., Papadopoulos J.: Planar sliding with dry friction. Part 1. Limit surface and moment function. Wear 143, 1991, 307-330.
7. Kikuuwe R., Takesue N., Sano A., Mochiyama H., Fujimoto H.: Fixed-step friction simulation: from classical Coulomb model to modern continuous models. In Proceedings of IEEE/RSJ International Conference on Intelligent Robots and Systems, Edmonton, Canada, 2005, 3910-3917.
8. Mason, M.T.: Progress in nonprehensile manipulation. The International Journal of Robotics Research 18, 1999, 1129-1141.
9. Piatkowski T.: Active fence with flexible link. Journal of Theoretical and Applied Mechanics 48, 2010, 87-109.
10. Piatkowski T., Sempruch J.: Model of inelastic impact of unit loads. Packaging Technology and Science 22, 2009, 39-51.
11. Piatkowski T., Sempruch J.: Model of the process of load unit stream sorting by means of flexible active fence. Mechanism and Machine Theory 43, 2008, 549-564.
12. Piatkowski T., Sempruch J.: Sorting process of load units – dynamic model of scraping process. The Archive of Mechanical Engineering 49, 2002, 23-46.
13. Root D.: Lansmont six-step method for cushioned package development. Package Dynamics Testing Laboratory, Lansmont Inc., Monterey, CA, USA, accessed 2010-07-15, www.lansmont.com/ SixStep/6stepPrint.htm.
14. Zienkiewicz O.C.: The finite element method. Butterworth-Heinemann, Oxford, UK, 2000.